

# Photosynthetic Vesicle Architecture and Constraints on Efficient Energy Harvesting

Melih Şener,<sup>†‡</sup> Johan Strümpfer,<sup>†§</sup> John A. Timney,<sup>¶</sup> Arvi Freiberg,<sup>||\*\*</sup> C. Neil Hunter,<sup>¶</sup> and Klaus Schulten<sup>†‡§\*</sup>

<sup>†</sup>Beckman Institute for Advanced Science and Technology, <sup>‡</sup>Department of Physics, and <sup>§</sup>Center for Biophysics and Computational Biology, University of Illinois at Urbana-Champaign, Urbana, Illinois; <sup>¶</sup>Department of Molecular Biology and Biotechnology, University of Sheffield, Sheffield, United Kingdom; and <sup>||</sup>Institute of Physics and <sup>\*\*</sup>Institute of Molecular and Cell Biology, University of Tartu, Tartu, Estonia

**ABSTRACT** Photosynthetic chromatophore vesicles found in some purple bacteria constitute one of the simplest light-harvesting systems in nature. The overall architecture of chromatophore vesicles and the structural integration of vesicle function remain poorly understood despite structural information being available on individual constituent proteins. An all-atom structural model for an entire chromatophore vesicle is presented, which improves upon earlier models by taking into account the stoichiometry of core and antenna complexes determined by the absorption spectrum of intact vesicles in *Rhodobacter sphaeroides*, as well as the well-established curvature-inducing properties of the dimeric core complex. The absorption spectrum of low-light-adapted vesicles is shown to correspond to a light-harvesting-complex 2 to reaction center ratio of 3:1. A structural model for a vesicle consistent with this stoichiometry is developed and used in the computation of excitonic properties. Considered also is the packing density of antenna and core complexes that is high enough for efficient energy transfer and low enough for quinone diffusion from reaction centers to cytochrome *bc*<sub>1</sub> complexes.

## INTRODUCTION

Photosynthesis provides energy for nearly all life on Earth, converting short-lived electronic excitation resulting from absorbing solar energy into increasingly more stable forms of energy, culminating in the production of ATP (1–7). In purple bacteria, this conversion process is performed by (pseudo-) organelles consisting of up to hundreds of proteins cooperating in a multistep process of light absorption, energy transfer (8–12), charge separation (13), quinone diffusion (14,15), and ATP synthesis (16,17).

The molecular assembly that performs light-harvesting is significantly simpler in the primitive purple bacteria than in their cyanobacterial or plant counterparts (1,18,19). In the purple bacterium *Rhodobacter (Rba.) sphaeroides* the photosynthetic apparatus is organized into chromatophore vesicles of nearly spherical shape of ~60 nm diameter. Membrane proteins that constitute most of a chromatophore vesicle are the reaction center-light-harvesting complex 1-PufX (RC-LH1-PufX) dimeric core complex, light-harvesting complex 2 (LH2), cytochrome *bc*<sub>1</sub> complex, and the ATP synthase. Structural models for these complexes have been known for some time for several species (20–33). The relative spatial arrangement of light-harvesting complexes in several bacterial photosynthetic membrane patches have been determined by atomic force microscopy (34–40) (AFM). In particular, the organization of *Rba. sphaeroides* chromatophores has been determined, in this case by a combination of fluorescence yield (41,42), linear dichroism, AFM (34,35), and cryo-electron microscopy (33,43,44) studies.

The aforementioned structural data have been combined recently into a comprehensive all-atom model of chromatophore vesicles (3,45). This model reveals the basis of efficient light-harvesting and energy transfer across an entire vesicle. However, recent developments necessitate a revision of this vesicle model. Determination of the overall molecular shape of the RC-LH1-PufX dimer showed that the two halves of the dimer are inclined toward each other at an angle of 146° on the periplasmic side of the complex (46). A detailed modeling study has explored the membrane-bending effects of this complex (47). Finally, a recent AFM study of membranes composed solely of the LH2 antenna has revealed the intercomplex spacings and membrane packing for this membrane protein (48). Taken together, one can now construct a model of the intracytoplasmic membrane (ICM) vesicle that takes into account the long-range membrane-bending effect of arrays of core dimers as well as the LH2-LH2 associations.

The results of this study are twofold. First, a new all-atom structural model for a chromatophore vesicle is presented based on the stoichiometry of core and antenna complexes determined by the absorption spectrum of intact low-light-adapted ( $< 100 \mu\text{E m}^{-2} \text{s}^{-1}$ ) vesicles from *Rba. sphaeroides*. The stated light intensity and the associated stoichiometry correspond to physiologically relevant growth conditions. The resulting all-atom vesicle model improves upon our earlier models (45), incorporating also a recent structural model for the membrane-bending core dimer complex based on a molecular dynamics-flexible fitting study (47,49). The resulting vesicle model is subsequently used to compute the overall excitation migration characteristics (45). Second, consistent with spatial constraints posed on the chromatophore vesicle architecture by the condition of efficient energy

Submitted November 24, 2009, and accepted for publication April 5, 2010.

\*Correspondence: kschulte@ks.uiuc.edu

Editor: Reinhard Lipowsky.

© 2010 by the Biophysical Society  
0006-3495/10/07/0067/9 \$2.00

doi: 10.1016/j.bpj.2010.04.013

transfer, a family of chromatophore models is generated from the aforementioned new vesicle model. The resulting energy transfer rates determine the limits posed on intercomplex separation that need to be wide enough to facilitate diffusion of quinones (48,50,51) on the one hand and narrow enough to maintain efficient light-harvesting on the other hand. Physics-based design constraints on the spatial arrangement of constituent components have been suggested earlier to be responsible in shaping the evolution of photosynthetic systems (19,52,53).

The organization of this article is as follows. In the next section the growth and spectroscopy of intact *Rba. sphaeroides* chromatophore vesicles are outlined, followed by the computation of energy transfer characteristics of the vesicles. Next, the stoichiometry of core and antenna complexes is determined from the absorption spectrum of vesicles grown under low light conditions. Then, excitation transfer rates between individual pairs of LH1-LH1, LH2-LH1, and LH2-LH2 complexes are presented as a function of spatial arrangement. Finally, the all-atom structural model for a new vesicle model is introduced along with the dependence of light-harvesting efficiency on the protein packing density.

## METHODS

In this section, a brief summary is presented: first, for the growth and subsequent spectroscopy of chromatophore vesicles, and second, for the computation of energy transfer rates between light-harvesting complexes according to an effective Hamiltonian formulation.

### Growth and spectroscopy of chromatophore vesicles

Cell cultures of *Rba. sphaeroides* 2.4.1 were grown photosynthetically under low light illumination ( $100 \mu\text{E m}^{-2} \text{s}^{-1}$ ) in M22+ liquid medium (54). Cells were subsequently lysed by French pressing at 18,000 psi. ICM vesicles were isolated from the resulting lysate by rate-zonal sucrose density gradient centrifugation (55). Membranes were harvested from the gradients and homogenized in 20 mM Tris buffer and 20% sucrose at pH 8.

Absorption spectra in buffer solutions of low light chromatophores and RC-LH1 complexes were measured at ambient temperature using a model No. V-530 spectrophotometer with spectral resolution of 0.5 nm (JASCO, Tokyo, Japan). Spectral adjustment involved a red shift and an intensity variation of the RC-LH1 spectrum with respect to the low-light-vesicle spectrum.

To determine the LH2:RC stoichiometry, the absorbance values at 850 nm for the deconvoluted LH2 spectrum (green in Fig. 1) and at 875 nm for the LH1 spectrum (red in Fig. 1) were used. The LH2-850:LH1-875 nm absorbance ratio (indicated by vertical line segments in Fig. 1) is 2.73. The absorbance values, divided by the appropriate extinction coefficients for the LH2 and LH1 complexes, reported as  $170 \pm 5$  and  $118 \pm 5 \text{ mM}^{-1} \text{ cm}^{-1}$ , respectively (56), yield in this membrane sample a ratio for the B850 (LH2):B875 (LH1) bacteriochlorophylls (BChls) of 1.9.

One dimeric RC-LH1-PufX complex contains 56 BChls absorbing in the 875-nm band and an LH2 complex contains 18 BChls absorbing in the 850-nm band; thus, a 1:1 LH2: RC-LH1-PufX dimer ratio (and therefore a 0.5 LH2:RC ratio) corresponds to a B850:B875 BChl ratio of 18:56, i.e., of 0.32, and a B850:B875 absorbance ratio of 0.46, once the higher extinction coefficient of B850 BChls is taken into account. The observed B850:B875 absorbance ratio of 2.73 taken from the deconvoluted absorbance spectrum

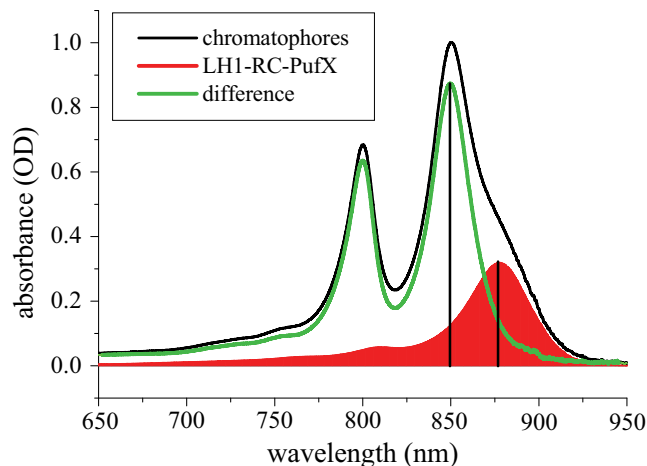


FIGURE 1 Absorption spectrum of chromatophores grown under low-light intensity (black line). Shown as a red solid area is an absorption spectrum of RC-LH1-PufX complexes adjusted under the absorption contour of chromatophores. The difference between the spectra for the entire chromatophore and for the RC-LH1-PufX complexes corresponds to the spectrum of LH2 complexes (green line). The ratio of absorbance maxima (indicated by vertical line segments) for the deconvoluted B850 and B875 components of LH2 and RC-LH1-PufX, respectively, is 2.73, from which an LH2:RC stoichiometry of 3:1 can be estimated (see Methods).

in Fig. 1, therefore, is equivalent to an LH2:RC ratio of  $(2.73/0.46) \times 0.5$ , i.e., of 3.

### Intercomplex energy transfer based on an effective Hamiltonian

The migration of energy across an entire chromatophore vesicle is described in terms of a sequence of transfer events between pairs of pigment clusters. The computation of energy transfer rates between two pigment clusters is based on an effective Hamiltonian formulation in the Förster formalism as recently reviewed in Şener and Schulten (3). We follow the formulation presented therein and, for the sake of completeness, present here a brief summary.

Single exciton-based effective Hamiltonians are defined in the basis set of the  $Q_y$ -excited states of BChls (57),

$$|i\rangle = |\phi_1 \phi_2 \dots \phi_i^* \dots \phi_N\rangle, \quad (1)$$

where the  $i^{\text{th}}$  BChl is in the electronically excited  $Q_y$ -state (3) and all other  $N-1$  BChls are in the ground state. In this basis set, the effective Hamiltonian is (6,58,59)

$$H = \sum_i \epsilon_i |i\rangle \langle i| + \sum_{i \neq j} V_{ij} |i\rangle \langle j|, \quad (2)$$

where  $\epsilon_i$  values are the BChl site energies and  $V_{ij}$  values account for the electronic coupling between sites. These quantities are usually determined to reproduce the observed spectral properties of the complex described in the literature (58,60). Effective Hamiltonians were successfully employed for the energy spectrum of purple bacterial light harvesting complexes (45,59,61–63).

Coupling  $V_{ij}$  between sufficiently separated BChls can be approximated by an induced dipole-induced dipole interaction (3)

$$V_{ij} = C \left( \frac{(\mathbf{d}_i \cdot \mathbf{d}_j)}{r_{ij}^3} - 3 \frac{(\mathbf{r}_{ij} \cdot \mathbf{d}_i)(\mathbf{r}_{ij} \cdot \mathbf{d}_j)}{r_{ij}^5} \right), \quad (3)$$

where  $\mathbf{d}_i$  values are the BChl (ground- $Q_y$ ) transition dipole unit vectors and  $C$  denotes the coupling strength depending on the complex to which the BChls belong (49,58–60).

The dipolar approximation (3) cannot be employed for closely spaced (<20 Å Mg-Mg distance) BChls such as the nearest neighbors in LH2 and LH1 or the special pair in the reaction center (RC). For such closely spaced BChls, couplings are determined typically through quantum chemistry calculations (64). In the following, we adopt site-energy and coupling parameters suggested in Şener and Schulten (3) and Şener et al. (49).

The rate of excitation transfer between two spatially separated BChl clusters can be approximated by the generalized Förster formula (2,3), which assumes that the donor cluster is thermodynamically equilibrated. i.e., transfer between acceptor and donor is followed by immediate thermal relaxation before subsequent transfer. A recent stochastic quantum mechanics study has revealed that LH2 exciton systems do indeed equilibrate within ~1 ps (65). Accordingly, the rate of transfer between a donor cluster  $D$  and an acceptor cluster  $A$  is

$$\mathcal{T}_{DA} = \frac{2\pi}{\hbar} \sum_{m \in D} \sum_{n \in A} \frac{e^{-E_m^D/k_B T}}{\sum_{l \in D} e^{-E_l^D/k_B T}} |V_{mn}^{DA}|^2 \int dE S_m^D(E) S_n^A(E). \quad (4)$$

Here  $E_m^D$ ,  $m = 1, 2, \dots$ , are the donor energy levels, and  $S_m^D(E)$  and  $S_n^A(E)$  are the donor and acceptor lineshapes, respectively. The coupling

$$V_{mn}^{DA} = \sum_{ij} c_{m,i}^D c_{n,j}^A V_{ij} \quad (5)$$

between donor state  $m$  and acceptor state  $n$  depends on the donor eigenvector  $c_{m,i}^D$  and the acceptor eigenvector  $c_{n,j}^A$  of the respective Hamiltonians defined in Kosztin and Schulten (2), where  $i$  and  $j$  span the BChls in the donor  $D$  and the acceptor  $A$  clusters, respectively. Lee et al. (66) recently reported observation of quantum coherence within a core complex of *Rba. sphaeroides* at cryogenic temperatures. At room temperature and for well-partitioned pigment aggregates such as the core and antenna complexes constituting a chromatophore vesicle, the generalized Förster formulation from Govindjee (4) yields results that compare closely with results from a more detailed stochastic quantum mechanics description (65) based on the hierarchy equation method originally proposed by Tanimura and Kubo (67).

The transition dipole moments of  $Q_y$ -excited states obey the sum rule of excitons (68)

$$\sum_{n=1}^N |\langle 0 | \mathbf{D} | \tilde{n} \rangle|^2 = \sum_{j=1}^N |\langle 0 | \mathbf{D} | j \rangle|^2 = N S_{\text{BChl}}, \quad (6)$$

where  $n$  and  $j$  span exciton states and BChl sites, respectively, and  $S_{\text{BChl}} = |\langle j | \mathbf{D} | 0 \rangle|^2$  is the oscillator strength of a single BChl, assumed to be uniform for all  $j$ , and  $|0\rangle$  denotes the ground state in which no BChl is excited.

Equation 4 permits computation of energy transfer rates across a network of hundreds of light harvesting proteins (45). To expedite this computation, lookup tables were constructed for pairwise transfer between core and antenna complexes within a cutoff distance of 300 Å. Tables were constructed for vesicle radii of 250 Å, 375 Å, and 500 Å; vesicles with intermediate radii were described through interpolation. The lookup tables enable rapid computation of excitonic properties based on the list of protein center positions and orientations.

The quantum yield  $q$  and average excitation lifetime  $\tau$  for a chromatophore vesicle are defined according to Şener and Schulten (3) in terms of the transition rates (4)

$$q = -k_{CS} \langle RC | K^{-1} | p(0) \rangle, \quad (7)$$

$$\tau = -\langle 1 | K^{-1} | p(0) \rangle, \quad (8)$$

where  $k_{CS}$  is the charge separation rate,  $|RC\rangle = \sum_i \delta_{i,RC} |i\rangle$  is given by a sum over all RCs,  $|1\rangle = \sum_i |i\rangle$ ,  $|p(0)\rangle$  is the initial state at  $t = 0$ , and the matrix  $K$  is defined in terms of the transition rates  $K_{ij} = T_{ji} - \delta_{ij} (\sum_k T_{ik} + k_{\text{diss}} + \delta_{i,RC} k_{CS})$ , where  $T$  is the matrix of transition rates (4) with  $i$  and  $j$  denoting specific donors and acceptors, and  $k_{\text{diss}}$  is the rate of dissipation (due to fluorescence and internal conversion) for excitons.

## RESULTS AND DISCUSSION

In this section, first, the absorption spectrum of chromatophore vesicles grown under low light conditions is presented. The absorption spectrum is used to determine the stoichiometry of LH2 and RC-LH1 complexes. Second, the dependence of energy transfer rates between pairs of pigment-protein complexes on their relative geometry is examined. Third, a novel model of chromatophore vesicle architecture is presented based on available data. The excitonic properties of vesicles with various packing densities are examined to determine geometry-based constraints on efficient energy harvesting.

### Absorption spectrum and stoichiometry of vesicles grown at low light intensity

The absorption spectrum of low-light-adapted ( $100 \mu\text{E m}^{-2} \text{s}^{-1}$ ) chromatophores is shown in Fig. 1 in comparison to the absorption spectrum of pure RC-LH1 complexes. The difference between the spectra for the entire chromatophore and for the RC-LH1-PufX complexes corresponds to the spectrum contributed by LH2 complexes. (The dimeric RC-LH1-PufX contains 64 BChls: 4 BChls in each RC and 56 BChls absorbing in the 875-nm band; the LH2 complex contains 27 BChls: 18 BChls absorbing in the 850-nm band and 9 BChls absorbing at 800 nm.) A comparison of the spectral intensities for the LH2 complexes with those of the RC-LH1-PufX complexes in the spectral range between 700 and 950 nm can be used to identify the LH2:RC stoichiometry. Taking into account the sum rule for exciton spectra (6), the absorption spectrum in Fig. 1 yields a ratio of maximum absorbance values for the deconvoluted B850 and B875 components of 2.73, corresponding to an LH2:RC stoichiometry of ~3:1 (see Methods). Under high light conditions ( $1100 \mu\text{E m}^{-2} \text{s}^{-1}$ ) a similar analysis of the absorption spectrum (not shown) reveals an LH2:RC stoichiometry of ~1:1.

Two earlier vesicle models presented in Şener et al. (45) correspond to LH2:RC stoichiometries of 2.8:1 and 8:1, suggested then for high light and low light conditions, respectively. Thus, we observe that the earlier all-atom model intended for high light in Şener et al. (45) actually corresponds approximately to low-light-grown vesicles in terms of stoichiometry, whereas the low-light-vesicle model (8:1 LH2:RC stoichiometry) presented in that same article (45) does not correspond to the growth conditions used in our laboratory cultures. It is possible that such a high LH2:RC stoichiometry may be realized by extreme low-light

conditions where extended LH2-only regions are beneficial. Even though the inclusion of such LH2-only regions in a chromatophore vesicle would decrease the overall quantum yield slightly due to increased average path length to RCs, the increased overall absorption cross section of the vesicle would more than compensate the lowering of the quantum yield.

In the following, the observed LH2:RC stoichiometry of 3:1 for low-light vesicles is assumed in the construction of a new all-atom model for a chromatophore vesicle based on the global structural motifs discussed in Şener et al. (45) as determined by AFM, electron microscopy, and linear dichroism studies (31–35,43,44,69), (such as the vertical North-South stacking (34,35) of RC-LH1 dimers). Furthermore, an average LH2-LH2 center-to-center distance of 85 Å (as measured between the cylindrical symmetry axes of the LH2 complexes) is adopted using the method of Olsen et al. (48), taking into account overpacking artifacts of the LH2 lattice during the preparation of vesicle samples for AFM imaging.

### Energy transfer rates between light-harvesting complexes as a function of geometry

The energy transfer between individual pigments over distances  $>10\text{--}20$  Å is dominated by the induced dipole-induced dipole coupling (3), which results in a  $1/r^6$  decay of transfer rates (11) (see Methods). The Förster radius between two pigments, defined as the distance over which the transfer efficiency is 0.5, is  $\sim 90$  Å for BChls. This permits a rather wide separation between two BChls before the probability of dissipation (rate  $\sim 1/\text{ns}$ ) becomes significant during excitation transfer. Over a network of thousands of BChls as found in a chromatophore vesicle (45), the migration of excitation is a Markovian process. The path length of an excitation within an antenna complex located peripherally with respect to a RC may be long enough to bring about a significant dissipation probability. Therefore, each light harvesting complex is required to be efficiently coupled to at least some neighboring complexes for rapid transfer of excitation to a RC. Furthermore, any photosynthetic species is under selective evolutionary pressure to achieve high efficiency of light harvesting (70), which may further constrain the permitted range of energy loss due to slow transfer between complexes in a vesicle. In the following, we examine how intercomplex separation affects energy transfer efficiency between pairs of core and antenna complexes.

The energy transfer times among the LH2-LH2, LH2-LH1, and LH1-LH1 pairs are shown in Fig. 2 *a* as a function of edge-to-edge distance between proteins (as measured from closest steric contact). The LH2 orientation in the plane of the membrane is found to be largely immaterial for energy transfer and, therefore, the LH2 complexes are treated as isotropic in their placement. This orientation-insensitivity

of transfer times may be an important structural theme for chromatophore vesicles because it permits the building of large excitation energy transfer arrays using repeated circular units without the need for a specific fit among the complexes. For LH2-LH1 and LH1-LH1 transfer a particular orientation of proteins (along the core dimer axis) is adopted in Fig. 2 *a*. The rates of transfer are notably similar for all pairings regardless of the type of complex when viewed as a function of edge-to-edge separation between proteins (for two LH2 proteins, steric contact corresponds to a center-to-center separation of  $\sim 80$  Å). Transfer times start at  $\leq 10$  ps for direct contact (corresponding to a nearest BChl-BChl separation of  $\sim 25$  Å), increasing quickly as complexes separate. Edge separation is defined through the closest sterically permitted placement of the corresponding proteins. It has been reported that excitation transfer in LH2-membranes exhibits also fast components down to 1-ps timescales (71). These fast transfer events are likely the result of the spectral inhomogeneity of the LH2 complexes across the membrane. To account for this spectral inhomogeneity and its effect on excitation transfer, thermal disorder effects (59) need to be modeled on the scale of an entire chromatophore vesicle, which is beyond the scope of this study.

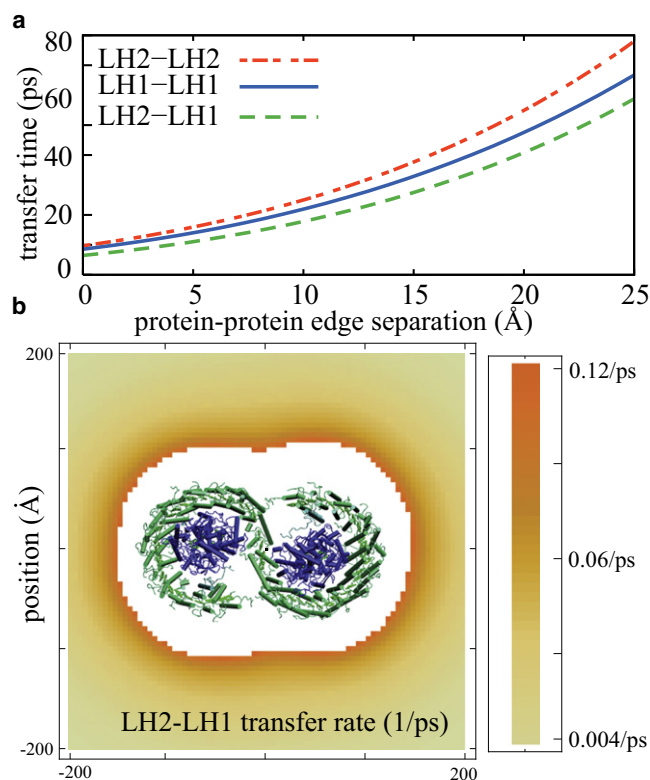


FIGURE 2 Excitation transfer time as a function of intercomplex separation. (a) Shown are LH2-LH2 (red), LH2-LH1 (green), and LH1-LH1 (blue) excitation transfer times as a function of edge-to-edge distance between proteins. (b) LH2-LH1 transfer times as a function of LH2 center position with respect to the dimerization axis of the RC-LH1-PufX complex. (White area at the center). Sterically excluded region for the placement of the LH2 center.

The transfer times more than double to 20 ps already at a separation of 10 Å. However, this does not immediately imply a significant loss of transfer efficiency as the dissipation timescale of 1 ns is significantly longer. Only through the collective effect of excitation transfer over many complexes does a significant loss due to dissipation accrue and lower the overall quantum-yield.

The energy transfer rate between LH2 and LH1 complexes for a planar arrangement is shown in Fig. 2 *b* as a function of the LH2 center location around an RC-LH1-PufX dimer. As can be seen by the contours of equal transfer rates, the transfer rate depends almost solely on the edge-to-edge separation and not on the relative placement of LH2 with respect to LH1. Steric hindrance between the two proteins limits the closest distance permitted for interprotein BChl separation. For such separated BChl clusters, the dipolar approximation is sufficiently accurate for interprotein pigment couplings. Furthermore, interprotein excitation transfer is slow enough compared to the thermal equilibration of exciton states determined in Strümpfer and Schulten (65) that the generalized Förster approximation (4) remains relevant.

The transfer efficiency between two complexes remains high (>0.9) even across a 25 Å separation. The results presented in the following section illustrate that, when a network of many complexes is considered, the demand of high transfer efficiency permits a much smaller average separation between proteins than demanded only by a single pair of proteins.

### All-atom structural model for a low-light-adapted chromatophore vesicle

The construction of atomistic models for the chromatophore vesicles of *Rba. sphaeroides* presented in Şener et al. (45) contained shortcomings that we address below. First, the vesicle models in Şener et al. (45), in the absence of accurate structural data, were constructed using planar RC-LH1-PufX dimer core models. Such a flat (as opposed to membrane-bending) core model distorts the curvature inherent in the pseudo-spherical vesicles of *Rba. sphaeroides*. Second, the assumed stoichiometry values for the LH2:RC ratios were inappropriate as mentioned above. Third, the packing density of LH2 units inaccurately reflected the overpacking during sample preparation for AFM imaging as discussed in Olsen et al. (48). We improve here upon the models in Şener et al. (45) by building a chromatophore vesicle that, on the one hand, replaces the earlier flat models of the core dimer with the recent membrane-bending structural model (49) and, on the other hand, adopts a stoichiometry consistent with the absorption spectrum of low-light-adapted vesicles (compare to Fig. 1), while maintaining a realistic LH2 packing density. Fourth, we assume a vesicle inner diameter of 55 nm as opposed to the diameter of 60 nm used in Şener et al. (45). Fifth, the current vesicle adopts the slanted vertical stacking of core dimers suggested in Qian et al.

(46) and Hsin et al. (47). The other structural motifs in Şener et al. (45) for core and antenna complex placement have been preserved in this study.

The chromatophore vesicle model thus constructed is shown in Fig. 3. The vesicle shown forms a closed sphere, i.e., not open at the South Pole corresponding to an attachment to the ICM as considered in Şener et al. (45). The topology of vesicles (i.e., closed spheres versus open invaginations of the ICM) is currently under debate and likely varies between species. It was recently reported that in *Phaeospirillum molischianum* ICM vesicles are continuously attached to the cell membrane (72). Furthermore, early studies of *Rba. sphaeroides* membranes (73) showed that the ICM in whole cells is accessible to the external environment (without determining the extent of accessibility). Cryo-electron tomography studies of *Rba. sphaeroides* ICM vesicles indicate the presence of both closed and open vesicles concurrently (74). We note that the excitonic properties considered in this study are largely independent of the vesicle topology.

No attempt has been made to model the location of an ATP synthase or of *bc*<sub>1</sub> complexes associated with the chromatophore as our current focus is on excitation migration properties. The vesicle model shown in Fig. 3 consists of 13 RC-LH1-PufX core dimers and 82 LH2 antenna complexes, corresponding to an LH2:RC stoichiometry of 3.15:1, close to the stoichiometry of 3:1 determined from the absorption spectrum given in Fig. 1.

The spherical shape of the vesicle necessitates the presence of gaps between the constituent proteins due to shape and curvature mismatch, the gaps facilitating quinone diffusion. Frese et al. (75) pointed out that such a mismatch of the local curvature profiles causes domain separation between different constituent proteins. In planar membranes, regular hexagonal lattices of LH2 complexes supposedly hinder quinone diffusion due to percolation effects (39). Such regular LH2 lattices are necessarily absent in a spherical vesicle geometry as a spherical region cannot be tiled by a regular hexagonal lattice. It was reported in Liu et al. (51) for *Rhodospirillum photometricum* membranes that size mismatch between core and antenna complexes contributes significantly to the presence of long-range diffusion networks for quinones; a protein concentration near the percolation threshold disrupts such networks (50).

The energy migration properties of a vesicle containing 3046 BChls, namely the one shown in Fig. 3, *a* and *b*, have been determined following the procedure in Şener et al. (45,49). The overall light-harvesting quantum yield of the vesicle is strongly dependent on the forward (LH1 → RC) transfer rate of excitations in the core complex (45). We choose this rate to be 1/(35 ps) to reproduce the observed average excitation lifetime (8) of 50 ps for core complexes (76). (In (45) a forward transfer rate of 1/(20 ps) was employed corresponding to slightly lower lifetimes and a slightly higher quantum yield.) The resulting quantum yield

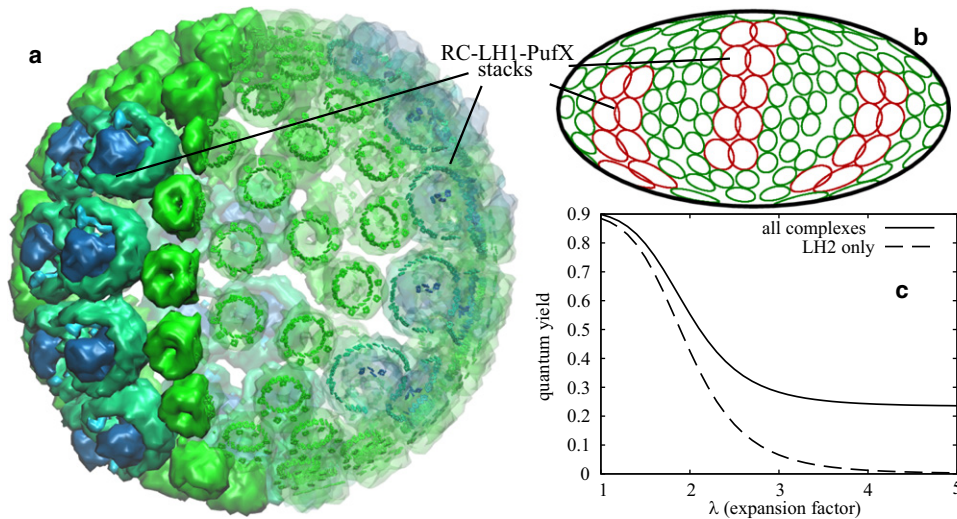


FIGURE 3 Chromatophore vesicle. (a) The low-light-adapted chromatophore vesicle is displayed in terms of BChls represented by their porphyrin rings and in terms of the constituent proteins in surface representation. The LH2:RC stoichiometry of 3.15 corresponds approximately to that determined by the absorption spectrum shown in Fig. 1. (b) The planar projection of core and antenna complexes based on the area preserving inverse-Mollweide map (45) (S-shaped RC-LH1 core dimers are represented as two overlapping red circles). (c) Quantum yield ( $\eta$ ) of vesicles as a function of expansion factor  $\lambda$  (see text).

for the entire vesicle is computed to be 90%, corresponding to an average excitation lifetime of 101 ps. This computed lifetime overestimates reported values of 60–80 ps (76–82). The difference may be partially due to the inaccuracy of the model and of the associated parameters outlined above as well as differences in vesicle composition. The low-light-vesicle model presented herein is likely to have a greater average excitation lifetime and a slightly lower corresponding quantum yield than a high-light-adapted vesicle.

### Light-harvesting efficiency and protein packing density

To examine the effects of intercomplex separation on the overall quantum yield, we consider an ensemble of vesicles of different radii from that shown in Fig. 3 a. For the purpose of generating respective vesicles, each core and antenna complex is translated along the vector connecting the vesicle center to the center of mass of the protein. In other words, for each complex  $i$  the center of mass position  $\mathbf{r}_i$  of each protein is multiplied by an expansion factor  $\lambda$  (i.e.,  $\mathbf{r}_i \rightarrow \lambda\mathbf{r}_i$ ), where  $\lambda \geq 1$ . Individual proteins are not enlarged or distorted during this process of translation. The relative orientation of each protein is also left unchanged. We note that the expansion of the vesicle by  $\lambda$ , as described, does not represent a biologically realistic process, but serves solely to enable a theoretical study of the role of protein density on light harvesting efficiency.

The excitonic properties and the quantum yield of the vesicles in the ensemble, corresponding to different expansion factors  $\lambda$ , were computed with the use of lookup tables for the generalized Förster transfer formula (4) introduced in Methods. As seen in Fig. 3 c, the quantum yield of excitations originating in antenna (LH2) complexes drops rapidly ( $<0.5$ ) as the expansion factor  $\lambda$  exceeds 1.8. Compared to the transfer of energy between a pair of complexes, the overall energy transfer efficiency of an entire vesicle is more

sensitive to intercomplex separation, i.e., to the packing density of the light-harvesting complexes.

For the stoichiometries considered in this study, most LH2 units neighbor RC-LH1 core complexes (only 32 of the 82 LH2 complexes did not have a core complex as an immediate neighbor; under higher light conditions this ratio becomes smaller as the density of core complexes increases). Therefore, efficiency loss in such a vesicle is dominated more strongly by LH2  $\rightarrow$  LH1 transfers than by LH2  $\rightarrow$  LH2 transfers. Thus, under corresponding light conditions, overall efficiency of the vesicle is dependent less on the average LH2-LH2 separation than on the average LH2-LH1 separation. Under extreme low-light conditions where there are large LH2-only domains, this argument is likely no longer valid.

### CONCLUSIONS

Purple bacterial chromatophore vesicles display remarkable simplicity in their architecture utilizing modularity both in the assembly of individual light-harvesting complexes from identical subunits and in the formation of vesicles from identical proteins. Light-harvesting complexes display a dual function, facilitating, in addition to their function of energy absorption and transfer, a curvature-induced clustering and subsequent invagination of vesicles (75). The theoretical basis for this kind of membrane sculpting via curvature-mediated interactions between proteins has been investigated in Reynwar et al. (83) and Cooke and Deserno (84).

The photosynthetic function involves a set of biophysical processes to be performed in parallel: light absorption, excitation transfer, charge separation, electron transfer from RCs to the  $bc_1$  complex by quinone diffusion, formation of a proton gradient, and utilization of the proton gradient for ATP synthesis. Some of these processes compete against one another for optimization of the vesicle geometry. For example, energy transfer is more efficient with closely packed light-harvesting complexes whereas quinone

diffusion is difficult in a tight lattice of LH2s (39). Also, the constituent proteins of a vesicle other than light-harvesting complexes (i.e., proteins not modeled in this study) likely induce gaps that lower energy transfer efficiency. However, as long as light-harvesting proteins are not spatially segregated from RC complexes by non-light-harvesting proteins, the overall reduction in light-harvesting efficiency is likely small enough not to be rate-limiting.

It is not fully understood how the competing demands of tight packing for efficient light-harvesting and loose packing for quinone diffusion are balanced in a functional vesicle, which furthermore must maintain its effectiveness under varying growth-conditions, i.e., for different protein stoichiometries. Chromatophore vesicles likely have lifetimes that are comparable to the lifetime of an individual bacterium. During the lifetime of a vesicle its components may need to be maintained and repaired. For example, radiation likely damages LH1 and LH2; their modular architectures would permit replacement of subunits, but the repair mechanism is not known. In addition, a closed spherical vesicle with only one ATP synthase will become defunct if its ATP synthase is degraded. A closed vesicle without an ATP synthase will be nonfunctional from its inception. Given that an average cell has hundreds of vesicles, there is likely some tolerance for defunct vesicles, but efficiency and optimality pressures of evolution would require mechanisms for the control of stoichiometry of vesicles during their assembly as well as mechanisms for repair and maintenance during their lifetime.

In this study we examined a key constraint acting upon photosynthetic vesicle architecture: efficient energy harvesting. The separation permitted between neighboring complexes to achieve sufficiently efficient energy transfer grants a wide enough gap between proteins for quinone diffusion. For efficient energy harvesting, it is not necessary that all light-harvesting complexes are tightly coupled to many neighbors, but rather it is sufficient that there exists at least one unbroken chain of excitonic couplings from any peripheral light-harvesting complex to a RC (i.e., the light-harvesting complex is not isolated amid non-light-harvesting proteins). The spherical geometry along with size mismatches of the proteins demand geometry irregularities, which may be a welcome feature in facilitating quinone diffusion (51).

LH2-minus mutants form vesicles in the form of tubules consisting of regular cylindrical arrays of RC-LH1 dimers with no gap for a possible  $bc_1$  complex in-between (47). If functional, these elongated vesicles would require quinones to travel large distances to  $bc_1$  complexes that are likely located at the membrane junction between vesicles and the bacterial inner membrane, although the requirement is alleviated by use of a quinone pool. If such long-distance diffusion takes place, then RC-LH1 dimer stacks (shown in Fig. 3) should permit a diffusion of quinones along their vertical axis. Future models of chromatophore vesicles need to identify the location of  $bc_1$  complexes that are

missing in the current models, to accurately account for the needed quinone diffusion process.

The challenge posed for this article's focus on the photosynthetic vesicles is to grasp how nature learned to reconcile the competing demands of overall vesicle function, the demands of effective assembly, repair, and light-harvesting efficiency, as well as quinone traffic and the propagation of the proton motive force to the ATP synthase. Past efforts have focused mostly on individual proteins and their separate functions. The application of biochemical, structural, and computational methods can now be used to investigate the assembly, architecture, and concerted function of the purple bacterial photosynthetic apparatus as a whole.

Molecular images in this article were generated with VMD (85). The authors thank Jen Hsin for helpful discussions and Kōu Timpmann for preparing Fig. 1.

This work was supported by the National Science Foundation (grants No. MCB0744057 and No. PHY0822613 to K.S.), the National Institutes of Health (grant No. P41-RR05969 to K.S.), the Biotechnology and Biological Research Council, UK (grant to C.N.H.), and the Estonian Science Foundation (grant No. 7002 to A.F.).

## REFERENCES

- Cogdell, R. J., A. Gall, and J. Köhler. 2006. The architecture and function of the light-harvesting apparatus of purple bacteria: from single molecules to *in vivo* membranes. *Q. Rev. Biophys.* 39:227–324.
- Kosztin, I., and K. Schulten. 2008. Molecular dynamics methods for bioelectronic systems in photosynthesis. *In* Biophysical Techniques in Photosynthesis II. T. Aartsma and J. Matysik, editors. Springer, Dordrecht, The Netherlands.
- Şener, M. K., and K. Schulten. 2008. From atomic-level structure to supramolecular organization in the photosynthetic unit of purple bacteria. *In* The Purple Phototrophic Bacteria. C. N. Hunter, F. Daldal, M. C. Thurnauer, and J. T. Beatty, editors. Springer, New York.
- Govindjee. 2000. Milestones in photosynthesis research. *In* Probing Photosynthesis: Mechanisms, Regulation, and Adaptation. M. Yunus, U. Pathre, and P. Mohanty, editors. Taylor and Francis, New York.
- Blankenship, R. E. 2002. Molecular Mechanisms of Photosynthesis. Blackwell Science, Malden, MA.
- Hu, X., T. Ritz, ..., K. Schulten. 2002. Photosynthetic apparatus of purple bacteria. *Q. Rev. Biophys.* 35:1–62.
- Şener, M. K., and K. Schulten. 2005. Physical principles of efficient excitation transfer in light harvesting. *In* Energy Harvesting Materials. D. L. Andrews, editor. World Scientific, Singapore.
- Emerson, R., and W. Arnold. 1932. The photochemical reaction in photosynthesis. *J. Gen. Physiol.* 16:191–205.
- Oppenheimer, J. R. 1941. Internal conversion in photosynthesis. *Proc. Am. Phys. Soc. Phys. Rev.* 60:158.
- Arnold, W., and J. R. Oppenheimer. 1950. Internal conversion in the photosynthetic mechanism of blue-green algae. *J. Gen. Physiol.* 33:423–435.
- Förster, T. 1948. Intermolecular energy migration and fluorescence [Zwischenmolekulare energiewanderung und fluoreszenz]. *Ann. Phys. (Leipzig)*. 2:55–75.
- Dexter, D. 1953. A theory of sensitized luminescence in solids. *J. Chem. Phys.* 21:836–850.
- Marcus, R. A., and N. Sutin. 1985. Electron transfers in chemistry and biology. *Biochim. Biophys. Acta.* 811:265–322.
- Crofts, A. R., and C. A. Wraight. 1983. The electrochemical domain of photosynthesis. *Biochim. Biophys. Acta.* 726:149–185.

15. Xia, D., C.-A. Yu, ..., J. Deisenhofer. 1997. Crystal structure of the cytochrome *bc*<sub>1</sub> complex from bovine heart mitochondria. *Science*. 277:60–66.
16. Junge, W., H. Lill, and S. Engelbrecht. 1997. ATP synthase: an electrochemical transducer with rotary mechanics. *Trends Biochem. Sci.* 22:420–423.
17. Fillingame, R. H., W. Jiang, and O. Y. Dmitriev. 2000. Coupling H<sup>+</sup> transport to rotary catalysis in F-type ATP synthases: structure and organization of the transmembrane rotary motor. *J. Exp. Biol.* 203:9–17.
18. Xiong, J., W. M. Fischer, ..., C. E. Bauer. 2000. Molecular evidence for the early evolution of photosynthesis. *Science*. 289:1724–1730.
19. Şener, M. K., C. Jolley, ..., K. Schulten. 2005. Comparison of the light-harvesting networks of plant and cyanobacterial photosystem I. *Biophys. J.* 89:1630–1642.
20. Deisenhofer, J., O. Epp, ..., H. Michel. 1985. Structure of the protein subunits in the photosynthetic reaction centre of *Rhodospseudomonas viridis* at 3 Å resolution. *Nature*. 318:618–624.
21. McDermott, G., S. M. Prince, ..., N. W. Isaacs. 1995. Crystal structure of an integral membrane light-harvesting complex from photosynthetic bacteria. *Nature*. 374:517–521.
22. Karrasch, S., P. A. Bullough, and R. Ghosh. 1995. The 8.5 Å projection map of the light-harvesting complex I from *Rhodospirillum rubrum* reveals a ring composed of 16 subunits. *EMBO J.* 14:631–638.
23. Hu, X., D. Xu, ..., H. Michel. 1995. Predicting the structure of the light-harvesting complex II of *Rhodospirillum molischianum*. *Protein Sci.* 4:1670–1682.
24. Koepke, J., X. Hu, ..., H. Michel. 1996. The crystal structure of the light-harvesting complex II (B800–850) from *Rhodospirillum molischianum*. *Structure*. 4:581–597.
25. Conroy, M. J., W. H. Westerhuis, ..., M. P. Williamson. 2000. The solution structure of *Rhodobacter sphaeroides* LH1β reveals two helical domains separated by a more flexible region: structural consequences for the LH1 complex. *J. Mol. Biol.* 298:83–94.
26. Roszak, A. W., T. D. Howard, ..., R. J. Cogdell. 2003. Crystal structure of the RC-LH1 core complex from *Rhodospseudomonas palustris*. *Science*. 302:1969–1972.
27. Papiz, M. Z., S. M. Prince, ..., N. W. Isaacs. 2003. The structure and thermal motion of the B800–850 LH2 complex from *Rps. acidophila* at 2.0 Å resolution and 100K: new structural features and functionally relevant motions. *J. Mol. Biol.* 326:1523–1538.
28. Allen, J. P., G. Feher, ..., D. C. Rees. 1987. Structure of the reaction center from *Rhodobacter sphaeroides* R-26: the protein subunits. *Proc. Natl. Acad. Sci. USA*. 84:6162–6166.
29. Ermler, U., G. Fritsch, ..., H. Michel. 1994. Structure of the photosynthetic reaction center from *Rhodobacter sphaeroides* at 2.65 Å resolution: cofactors and protein-cofactor interactions. *Structure*. 2:925–936.
30. Camara-Artigas, A., D. Brune, and J. P. Allen. 2002. Interactions between lipids and bacterial reaction centers determined by protein crystallography. *Proc. Natl. Acad. Sci. USA*. 99:11055–11060.
31. Jamieson, S. J., P. Wang, ..., P. A. Bullough. 2002. Projection structure of the photosynthetic reaction centre-antenna complex of *Rhodospirillum rubrum* at 8.5 Å resolution. *J. Mol. Biol.* 21:3927–3935.
32. Fotiadis, D., P. Qian, ..., C. N. Hunter. 2004. Structural analysis of the reaction center light-harvesting complex I photosynthetic core complex of *Rhodospirillum rubrum* using atomic force microscopy. *J. Biol. Chem.* 279:2063–2068.
33. Qian, P., C. N. Hunter, and P. A. Bullough. 2005. The 8.5 Å projection structure of the core RC-LH1-PufX dimer of *Rhodobacter sphaeroides*. *J. Mol. Biol.* 349:948–960.
34. Bahatyrova, S., R. N. Frese, ..., C. N. Hunter. 2004. The native architecture of a photosynthetic membrane. *Nature*. 430:1058–1062.
35. Frese, R. N., C. A. Siebert, ..., R. van Grondelle. 2004. The long-range organization of a native photosynthetic membrane. *Proc. Natl. Acad. Sci. USA*. 101:17994–17999.
36. Scheuring, S., J. N. Sturgis, ..., J.-L. Rigaud. 2004. Watching the photosynthetic apparatus in native membranes. *Proc. Natl. Acad. Sci. USA*. 91:11293–11297.
37. Scheuring, S. 2006. AFM studies of the supramolecular assembly of bacterial photosynthetic core-complexes. *Curr. Opin. Struct. Biol.* 10:1–7.
38. Scheuring, S., R. P. Gonçalves, ..., J. N. Sturgis. 2006. The photosynthetic apparatus of *Rhodospseudomonas palustris*: structures and organization. *J. Mol. Biol.* 358:83–96.
39. Scheuring, S. 2008. The supramolecular assembly of the photosynthetic apparatus of purple bacteria investigated by high-resolution atomic force microscopy. In *The Purple Phototrophic Bacteria*. C. N. Hunter, F. Daldal, M. C. Thurnauer, and J. T. Beatty, editors. Springer, New York.
40. Sturgis, J. N., J. D. Tucker, ..., R. A. Niederman. 2009. Atomic force microscopy studies of native photosynthetic membranes. *Biochemistry*. 48:3679–3698.
41. Monger, T. G., and W. W. Parson. 1977. Singlet-triplet fusion in *Rhodospseudomonas sphaeroides* chromatophores. A probe of the organization of the photosynthetic apparatus. *Biochim. Biophys. Acta*. 460:393–407.
42. Hunter, C. N., H. J. M. Kramer, and R. van Grondelle. 1985. Linear dichroism and fluorescence emission of antenna complexes during photosynthetic unit assembly in *Rhodospseudomonas sphaeroides*. *Biochim. Biophys. Acta*. 807:44–51.
43. Jungas, C., J. L. Ranck, ..., A. Verméglio. 1999. Supramolecular organization of the photosynthetic apparatus of *Rhodobacter sphaeroides*. *EMBO J.* 18:534–542.
44. Siebert, C. A., P. Qian, ..., P. A. Bullough. 2004. Molecular architecture of photosynthetic membranes in *Rhodobacter sphaeroides*: the role of PufX. *EMBO J.* 23:690–700.
45. Şener, M. K., J. D. Olsen, ..., K. Schulten. 2007. Atomic-level structural and functional model of a bacterial photosynthetic membrane vesicle. *Proc. Natl. Acad. Sci. USA*. 104:15723–15728.
46. Qian, P., P. A. Bullough, and C. N. Hunter. 2008. Three-dimensional reconstruction of a membrane-bending complex: the RC-LH1-PufX core dimer of *Rhodobacter sphaeroides*. *J. Biol. Chem.* 283:14002–14011.
47. Hsin, J., J. Gumbart, ..., K. Schulten. 2009. Protein-induced membrane curvature investigated through molecular dynamics flexible fitting. *Biophys. J.* 97:321–329.
48. Olsen, J. D., J. D. Tucker, ..., C. N. Hunter. 2008. The organization of LH2 complexes in membranes from *Rhodobacter sphaeroides*. *J. Biol. Chem.* 283:30772–30779.
49. Şener, M. K., J. Hsin, ..., K. Schulten. 2009. Structural model and excitonic properties of the dimeric RC-LH1-PufX complex from *Rhodobacter sphaeroides*. *Chem. Phys.* 357:188–197.
50. Scheuring, S., and J. N. Sturgis. 2006. Dynamics and diffusion in photosynthetic membranes from *Rhodospirillum photometricum*. *Biophys. J.* 91:3707–3717.
51. Liu, L.-N., K. Duquesne, ..., S. Scheuring. 2009. Quinone pathways in entire photosynthetic chromatophores of *Rhodospirillum photometricum*. *J. Mol. Biol.* 393:27–35.
52. Noy, D., C. C. Moser, and P. L. Dutton. 2006. Design and engineering of photosynthetic light-harvesting and electron transfer using length, time, and energy scales. *Biochim. Biophys. Acta*. 1757:90–105.
53. Noy, D. 2008. Natural photosystems from an engineer's perspective: length, time, and energy scales of charge and energy transfer. *Photosynth. Res.* 95:23–35.
54. Hunter, C. N., J. D. Pennoyer, ..., R. A. Niederman. 1988. Oligomerization states and associations of light-harvesting pigment protein complexes of *Rhodobacter sphaeroides* as analyzed by lithium dodecyl sulfate-polyacrylamide gel electrophoresis. *Biochemistry*. 27:3459–3467.
55. Niederman, R. A., and K. D. Gibson. 1978. Isolation and physicochemical properties of membranes from purple photosynthetic bacteria. In

- The Photosynthetic Bacteria. R. K. Clayton and W. R. Sistrom, editors. MIT Press, Cambridge, UK.
56. Sturgis, J. N., C. N. Hunter, and R. A. Niederman. 1988. Spectra and extinction coefficients of near-infrared absorption bands in membranes of *Rhodobacter sphaeroides* mutants lacking light harvesting and reaction centre complexes. *Photochem. Photobiol.* 48:243–247.
  57. Scheer, H. 1991. Chlorophylls. CRC Press, Boca Raton, FL.
  58. Ritz, T., S. Park, and K. Schulten. 2001. Kinetics of excitation migration and trapping in the photosynthetic unit of purple bacteria. *J. Phys. Chem. B.* 105:8259–8267.
  59. Şener, M., and K. Schulten. 2002. A general random matrix approach to account for the effect of static disorder on the spectral properties of light harvesting systems. *Phys. Rev. E.* 65:031916.
  60. Damjanović, A., T. Ritz, and K. Schulten. 2000. Excitation energy trapping by the reaction center of *Rhodobacter sphaeroides*. *Int. J. Quantum Chem.* 77:139–151.
  61. Sundström, V., T. Pullerits, and R. van Grondelle. 1999. Photosynthetic light-harvesting: reconciling dynamics and structure of purple bacterial LH2 reveals function of photosynthetic unit. *J. Phys. Chem. B.* 103:2327–2346.
  62. Tretiak, S., C. Middleton, ..., S. Mukamel. 2000. Bacteriochlorophyll and carotenoid excitonic couplings in the LH2 system of purple bacteria. *J. Phys. Chem. B.* 104:9540–9553.
  63. Damjanović, A., I. Kosztin, ..., K. Schulten. 2002. Excitons in a photosynthetic light-harvesting system: a combined molecular dynamics, quantum chemistry and polaron model study. *Phys. Rev. E.* 65:031919.
  64. Cory, M. G., M. C. Zerner, ..., K. Schulten. 1998. Electronic excitations in aggregates of bacteriochlorophylls. *J. Phys. Chem. B.* 102:7640–7650.
  65. Strümpfer, J., and K. Schulten. 2009. Light harvesting complex II B850 excitation dynamics. *J. Chem. Phys.* 131:225101–225109.
  66. Lee, H., Y.-C. Cheng, and G. R. Fleming. 2007. Coherence dynamics in photosynthesis: protein protection of excitonic coherence. *Science.* 316:1462–1465.
  67. Tanimura, Y., and R. Kubo. 1989. Time-dependent spectrum of a two-level system coupled to a heat bath driven by pulsed laser. *J. Phys. Soc. Jpn.* 58:3001–3012.
  68. Hu, X., T. Ritz, ..., K. Schulten. 1997. Pigment organization and transfer of electronic excitation in the purple bacteria. *J. Phys. Chem. B.* 101:3854–3871.
  69. Frese, R. N., J. D. Olsen, ..., R. van Grondelle. 2000. The long-range supraorganization of the bacterial photosynthetic unit: a key role for PufX. *Proc. Natl. Acad. Sci. USA.* 97:5197–5202.
  70. Şener, M. K., D. Lu, ..., K. Schulten. 2002. Robustness and optimality of light harvesting in cyanobacterial photosystem I. *J. Phys. Chem. B.* 106:7948–7960.
  71. Timpmann, K., N. W. Woodbury, and A. Freiberg. 2000. Unraveling exciton relaxation and energy transfer in LH2 photosynthetic antennas. *J. Phys. Chem. B.* 104:9769–9771.
  72. Mascle-Allemand, C., J. Lavergne, ..., J. N. Sturgis. 2008. Organization and function of the *Phaeospirillum molischianum* photosynthetic apparatus. *Biochim. Biophys. Acta.* 1777:1552–1559.
  73. Francis, G. A., and W. R. Richards. 1980. Localization of photosynthetic membrane components in *Rhodospseudomonas sphaeroides* by a radioactive labeling procedure. *Biochemistry.* 19:5104–5111.
  74. Tucker, J. D., C. A. Siebert, ..., C. Neil Hunter. 2010. Membrane invagination in *Rhodobacter sphaeroides* is initiated at curved regions of the cytoplasmic membrane, then forms both budded and fully detached spherical vesicles. *Mol. Microbiol.* 76:833–847.
  75. Frese, R. N., J. C. Pàmies, ..., R. van Grondelle. 2008. Protein shape and crowding drive domain formation and curvature in biological membranes. *Biophys. J.* 94:640–647.
  76. Freiberg, A., J. P. Allen, ..., N. W. Woodbury. 1996. Energy trapping and detrapping by wild type and mutant reaction centers of purple non-sulfur bacteria. *Photosynth. Res.* 48:309–319.
  77. Sundström, V., R. van Grondelle, ..., T. Gillbro. 1986. Excitation-energy transport in the bacteriochlorophyll antenna systems of *Rhodospirillum rubrum* and *Rhodobacter sphaeroides*, studied by low-intensity picosecond absorption spectroscopy. *Biochim. Biophys. Acta Bioenerg.* 851:431–446.
  78. Borisov, A. Y., A. Freiberg, ..., K. Timpmann. 1985. Kinetics of picosecond bacteriochlorophyll luminescence in vivo as a function of the reaction center state. *Biochim. Biophys. Acta.* 807:221–229.
  79. Bergström, H., R. van Grondelle, and V. Sundström. 1989. Characterization of excitation energy trapping in photosynthetic purple bacteria at 77 K. *FEBS Lett.* 250:503–508.
  80. Visscher, K. J., H. Bergström, ..., R. van Grondelle. 1989. Temperature dependence of energy transfer from the long wavelength antenna Bchl-896 to the reaction center in *Rhodospirillum rubrum*, *Rhodobacter sphaeroides* (w.t. and M21 mutant) from 77 to 177 K, studied by picosecond absorption spectroscopy. *Photosynth. Res.* 22:211–217.
  81. Pullerits, T., K. J. Visscher, ..., R. van Grondelle. 1994. Energy transfer in the inhomogeneously broadened core antenna of purple bacteria: a simultaneous fit of low-intensity picosecond absorption and fluorescence kinetics. *Biophys. J.* 66:236–248.
  82. Timpmann, K., A. Freiberg, and V. Sundström. 1995. Energy trapping and detrapping in the photosynthetic bacterium *Rhodospseudomonas viridis*: transfer-to-trap-limited dynamics. *Chem. Phys.* 194:275–283.
  83. Reynwar, B. J., G. Illya, ..., M. Deserno. 2007. Aggregation and vesiculation of membrane proteins by curvature-mediated interactions. *Nature.* 447:461–464.
  84. Cooke, I. R., and M. Deserno. 2006. Coupling between lipid shape and membrane curvature. *Biophys. J.* 91:487–495.
  85. Humphrey, W., A. Dalke, and K. Schulten. 1996. VMD: visual molecular dynamics. *J. Mol. Graph.* 14:33–38, 27–28.